# Amylosucrase, a glucan-synthesizing enzyme from the $\alpha$-amylase family

Lars K. Skov, Osman Mirza, Anette Henriksen, Gabrielle Potocki de Montalk, Magali Remaud-Simeon, Patricia Sarcabal, Rene-Marc Willemot, Pierre Monsan, Mickael Gajhede

THE JOURNAL OF BIOLOGICAL CHEMISTRY
Vol. 276, No. 27, Issue of July 6, pp. 25273–25278, 2001

*Printed in U.S.A.*

# Amylosucrase, a Glucan-synthesizing Enzyme from the α-Amylase Family*

Received for publication, December 6, 2000, and in revised form, March 30, 2001
Published, JBC Papers in Press, April 16, 2001, DOI 10.1074/jbc.M010998200

**Lars K. Skov‡, Osman Mirza‡, Anette Henriksen‡§, Gabrielle Potocki De Montalk¶, Magali Remaud-Simeon¶, Patricia Sarçabal¶, Rene-Marc Willemot¶, Pierre Monsan¶, and Michael Gajhede‡‖**

*From the ‡Protein Structure Group, Department of Chemistry, University of Copenhagen, Universitetsparken 5, DK-2100 Copenhagen, Denmark and the ¶Département de Génie Biochimique et Alimentaire, Centre de BioIngéniere G. Durand, UMR CNRS 5504, UMR INRA 792, Institut National des Sciences Appliquees, Avenue de Rangueil, F-31077 Toulouse Cedex 4, France*

**Amylosucrase (E.C. 2.4.1.4) is a member of Family 13 of the glycoside hydrolases (the α-amylases), although its biological function is the synthesis of amylose-like polymers from sucrose. The structure of amylosucrase from *Neisseria polysaccharea* is divided into five domains: an all helical N-terminal domain that is not similar to any known fold, a $(\beta/\alpha)_8$-barrel A-domain, B- and B′-domains displaying α/β-structure, and a C-terminal eight-stranded β-sheet domain. In contrast to other Family 13 hydrolases that have the active site in the bottom of a large cleft, the active site of amylosucrase is at the bottom of a pocket at the molecular surface. A substrate binding site resembling the amylase 2 subsite is not found in amylosucrase. The site is blocked by a salt bridge between residues in the second and eight loops of the $(\beta/\alpha)_8$-barrel. The result is an exo-acting enzyme. Loop 7 in the amylosucrase barrel is prolonged compared with the loop structure found in other hydrolases, and this insertion (forming domain B′) is suggested to be important for the polymer synthase activity of the enzyme. The topology of the B′-domain creates an active site entrance with several ravines in the molecular surface that could be used specifically by the substrates/products (sucrose, glucan polymer, and fructose) that have to get in and out of the active site pocket.**

Amylosucrase (AS)[1] is a hexosyltransferase (E.C. 2.4.1.4) produced by non-pathogenic bacteria from the *Neisseria* genus and was identified in *N. perflava* as early as 1946 (1). MacKenzie *et al*. (2) identified intracellular AS in six other *Neisseriae* species, and later an extracellular *N. polysaccharea* AS was discovered (3). *N. polysaccharea* was isolated from the throats of healthy children, and it was suggested that the function of the secreted glucansucrase AS was to produce insoluble polymers. Until recently AS has only been found in bacteria from the *Neisseria* genus, but the *Deinococcus radiodurans* genome (4) and the *Caulobacter crescentus* genome (5) actually encodes proteins with a similar length that are 43 and 34%, respectively, identical to AS from *N. polysaccharea*.

In the presence of an activator polymer (*e.g.* glycogen), AS catalyzes the synthesis of an amylose-like polysaccharide composed of only α-(1→4)-glucosidic linkages using sucrose as the only energy source (6). This glycogen pathway is not found in *e.g. Escherichia coli*, which like most bacteria require activated α-D-glucosyl-nucleoside-diphosphate substrates for polysaccharide synthesis (7). The utilization of a readily available substrate makes AS a potentially very useful glucosylation tool for the production of novel amylopolysaccharides.

The recent cloning of *N. polysaccharea* AS in *E. coli* (8, 9) has made mutational (10) and detailed kinetic studies of highly purified enzyme possible (11, 12). It has also provided AS in sufficient amounts for successful crystallization experiments (13). The recombinant AS is derived from a glutathione *S*-transferase fusion protein and consists of a single polypeptide chain with 636 amino acid residues including 6 cysteines and 15 methionines.

Based on amino acid sequence comparisons, AS has been suggested to belong to the α-amylase superfamily, the α-retaining glycoside hydrolase (GH) Family 13 (14). Putative active site residues in the predicted $(\beta/\alpha)_8$-barrel have also been pointed out (9). Most members of this family hydrolyze α-(1→4) and α-(1→6)-glucosidic linkages of starch.

The α-amylase reaction mechanism is a general acid catalysis, similar to all of the glucoside hydrolases (16), and the same mechanistic scheme can also accommodate glucan synthesis from sucrose as shown in Scheme 1. The reaction is initiated by simultaneous protonation of the glycosidic bond by a proton donor and a nucleophilic attack on the anomeric carbon of the glucose moiety. This leads to the covalently linked substrate-enzyme intermediate. The intermediate can react with either water or with another saccharide molecule, as shown in the scheme. This implicates that the ratio between hydrolysis and transglycosylation is determined only by the relative concentrations of water and sugar moieties in the active site.

Consistent with Scheme 1, AS catalyzes both sucrose hydrolysis and oligosaccharide and polymer synthesis in the absence of an activator polymer (11). With 10 mM sucrose as the sole substrate, AS produces glucose (30%), maltose (29%), maltotriose (18%), turanose (11%), and insoluble polymer (12%).

Apart from AS, the GH Family 13 comprises other enzymes with non-hydrolytic functions. The crystal structure of a cyclo-

* This work was supported by the EU biotechnology project Alpha-Glucan Active Designer Enzymes (AGADE, BI04-CT98–0022) and the Danish Synchrotron User Center (DANSYNC). The costs of publication of this article were defrayed in part by the payment of page charges. This article must therefore be hereby marked "*advertisement*" in accordance with 18 U.S.C. Section 1734 solely to indicate this fact.

*The atomic coordinates and structure factors (code 1G5A) have been deposited in the Protein Data Bank, Research Collaboratory for Structural Bioinformatics, Rutgers University, New Brunswick, NJ (http://www.rcsb.org/).*

§ Present address: Dept. of Chemistry, Carlsberg Laboratory, Gamle Carlsberg Vej 10, DK-2500 Valby, Denmark.

‖ To whom correspondence should be addressed: Tel.: 45 35 32 02 80; Fax: 45 35 32 02 99; E-mail: gajhede@psg.ki.ku.dk.

[1] The abbreviations used are: AS, amylosucrase; GH, glycoside hydrolase; CGTase, cyclodextrin glucanotransferase; rms, root mean squared; MAD, multiple wavelength anomalous dispersion.

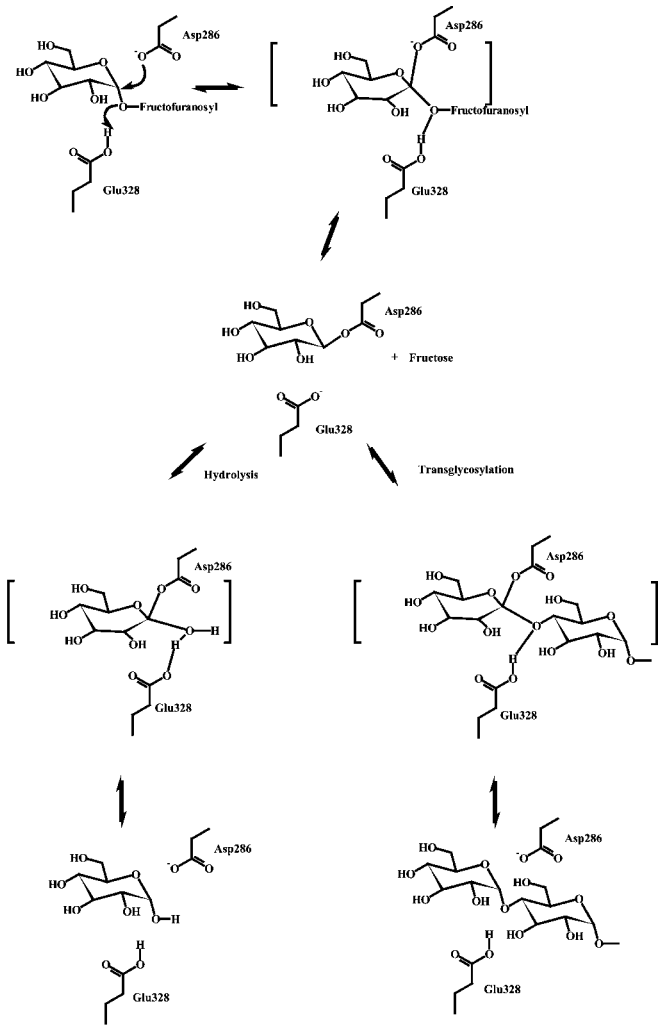


SCHEME 1. **General reaction mechanism for hydrolysis and transglycosylation.**

dextrin glucanotransferase (17) (CGTase) showed an active site architecture very similar to the α-amylase from *Aspergillus oryzae* (18) (TAKA-amylase, the first α-amylase structure determined) and thus implicated very similar reaction mechanisms at least for the formation of the covalent intermediate. The presence of a covalent intermediate has been verified experimentally in CGTases (19).

These findings all suggest that the active site of AS is highly similar to those of the α-amylases and CGTases. Structure determinations of complexes with substrate analogues have yielded detailed information on the α-amylase structure/function relationships. A stringent nomenclature for enzyme-substrate interactions has been developed, and substrate binding is usually described in terms of numbered sugar binding subsites (20). The catalytic residues are then located between the sugar binding subsites −1 and +1, when numbering the polysaccharide from the reducing end. In this work, we present the crystal structure of AS at a resolution of 1.4 Å, which represents the first crystal structure of a glucansucrase and is the first structure of a glucan-elongating enzyme from the GH 13 family. The structural alignment of AS and α-amylase-substrate analogue complexes is well suited to provide a basis for the understanding of product profile and substrate specificity observed for AS.

## EXPERIMENTAL PROCEDURES

*Crystallization*—Expression and purification of recombinant AS was performed as described previously (9, 12). The production of Se-Met AS and the crystallization conditions (equal amounts of 4 mg/ml protein solution (150 mM NaCl, 50 mM Tris-HCl, pH 7.0, 1 mM EDTA, and 1 mM α-dithiothreitol) and reservoir solution (30% polyethylene glycol $M_r$ 6000 and 0.1 M HEPES, pH 7.0)) have been published (13).

*Data Collection, Structure Determination, and Refinement*—All data were collected at the ESRF, Grenoble and were processed and scaled using DENZO and SCALEPACK (21). Multiple wavelength anomalous dispersion (MAD) data were collected at beamline BM 14. Data were collected using energies corresponding to the inflection point and peak of the experimentally determined selenium K edge and a remote high energy wavelength (Table I). All 15 selenium sites were identified when the MAD data were analyzed by the SOLVE program (22). Phases were extended to 1.7 Å using DM (23), and the structure was build with the automated tracing procedure ARP/wARP (24). This tracing located 625 of the total 628 amino acid residues found in the structure. Later a 1.4 Å native data set was obtained at beamline ID 14 EH 1 (λ = 0.934 Å), and the structure was refined at this level of resolution. Further rebuilding was done in program O (25), and refinement was performed with the CNS program package (26). A total of 628 amino acid residues, one Tris molecule, one HEPES molecule, a sodium ion, and 751 water molecules were included in the final model. Refinement statistics are listed in Table I. Several patches of elongated electron density that could arise from a polyethylene glycol molecule were not fitted. Thirty-one of the side chains were fitted with two conformations, and for sixteen surface side chains some of the outermost atoms displayed high B-factors. A polymerase chain reaction error was detected in the structure. Surface residue 537 was found to be an Asp/Asn instead of a Gly predicted by the sequence of the native enzyme. The nucleotide sequence of the recombinant DNA identified the residue as an Asp. The stereochemistry of the final model was analyzed by PROCHECK (27): 91% of the residues were found to lie in the most favorable regions of the Ramachandran plot and 8.6% in the additional allowed regions. Only two residues ($Glu^{344}$ and $Phe^{250}$) were found in a generously allowed region. A schematic representation of the enzyme is shown in Fig. 1. The overall B-factor for the protein is 16.4 $Å^2$, whereas it is 15.9 $Å^2$ and 16.5 $Å^2$ for the main chain and the side chain atoms, respectively. The B-factors of the Cα atoms are plotted in Fig. 2. The active site is shown in Fig. 3 as an example of the quality of the $1\sigma$ ($2F_o$-$F_c$) electron density.

*Coordinates*—Coordinates have been deposited at the Protein Data Bank (accession code 1G5A).

## RESULTS AND DISCUSSION

*Description of the Structure*—The single polypeptide chain (628 amino acid residues) is folded into a tertiary structure with five domains named N, A, B, B′, and C (Fig. 1). Residues 1–90 comprise the all α-helical N-domain. It contains six amphiphilic helices that we have chosen to name nh1 to nh6. The helices consist of the residues $Pro^2$–$Leu^{12}$, $Thr^{16}$–$Lys^{25}$, $Ser^{26}$–$Pro^{41}$, $Pro^{41}$–$Gly^{52}$, $Leu^{57}$–$Arg^{75}$, and $Ser^{77}$–$Asn^{88}$ as defined by the Kabsch-Sander algorithm (28) in the program PROCHECK (27). No known structures or domains were found to be similar to the AS N-domain in a database search with the DALI (29) server. Two helices from the N-domain (nh4 and nh5) are packed against two helices (h3 and h4) from the central $(\beta/\alpha)_8$-barrel (domain A) forming a four-helix bundle. The interface between the helices in the bundle is almost entirely hydrophobic, and no solvent molecules are located in the interface.

Domain A (residues 98–184, 261–395, and 461–550) is made up of eight alternating β-sheets (e1-e8) and α-helices (h1-h8) giving the catalytic core (the well characterized $(\beta/\alpha)_8$-barrel) common to the GH Family 13 (Figs. 1 and 4). A characteristic of the $(\beta/\alpha)_8$-barrel enzymes is that the loop region connecting strands to helices (labeled loop1 to loop8) are much longer on average than those connecting helices to strands. In particular AS has two loops (loop3 and loop7) that are so long that they constitute the separate domains B and B′. The positions of the secondary structural elements within the primary structure of domain A are shown in Fig. 4.

Domain B (residues 185–260) contains two short antiparallel β-sheets. The inner sheet (relative to the barrel) is formed by two strands (residues 187–190 and 253–256) and the outer sheet is formed by three strands (residues 211–213, 237–240, and 245–248) flanked by two α-helices (residues 193–201 and

TABLE I
*Data collection and refinement statistics*

| | | | | |
|---|---|---|---|---|
| Data collection | | | | |
| Protein | | Se-Methionine | | Native |
| Wavelength (Å) | 0.9788 | 0.9791 | 0.8857 | 0.934 |
| | Peak | Edge | Remote | |
| Unit cell (Å$^3$) | 95.9 × 116.5 × 60.5 | | | 95.7 × 117.1 × 61.0 |
| Space group | $P2_12_12$ | | | $P2_12_12$ |
| Resolution limit (Å)[a] | 2.8 (2.9–2.8) | 2.8 (2.9–2.8) | 2.8 (2.9–2.8) | 1.4 (1.45–1.4) |
| Observed reflections | 99,555 | 76,295 | 99,574 | 741,187 |
| Unique reflections | 28,081 | 22,143 | 26,222 | 127,114 |
| Completeness (%)[a] | 90.7 (86.5) | 71.5 (68.0) | 84.9 (93.4) | 93.9 (92.3) |
| $R_{sym}$ (%)[a,b] | 6.8 (11.4) | 6.8 (10.2) | 9.1 (15.0) | 17.4 (38.1) |
| Refinement statistics | | | | |
| $R_{cryst}/R_{free}$ (%)[c] | 18.9/20.4 | | | |
| Number of nonhydrogen atoms | | | | |
| Total | 5923 | | | |
| Protein | 5148 | | | |
| Water | 751 | | | |
| R.m.s. from ideal geometry | | | | |
| Bonds (Å) | 0.005 | | | |
| Angles (°) | 1.2 | | | |
| Average B factor (Å$^2$) | | | | |
| All atoms | 17.7 | | | |
| Protein | 16.4 | | | |
| TRIS | 15.2 | | | |
| HEPES | 32.8 | | | |
| Water | 22.3 | | | |
| Cross-validated estimated coordinate error | | | | |
| E.s.d. from Luzzati plot (Å) | 0.17 | | | |
| E.s.d. from Sigmaa (Å) | 0.10 | | | |

[a] Numbers in parenthesis are for the highest resolution shell.
[b] $R_{sym} = \Sigma_{hkl}(\Sigma_i(|I_{hkl,\,i} - \langle I_{hkl}\rangle|))/\Sigma_{hkl,\,i}\langle I_{hkl}\rangle$, where $I_{hkl,\,I}$ is the intensity of an individual measurement of reflection hkl and $\langle I_{hkl}\rangle$ is the mean intensity of that reflection.
[c] $R_{cryst} = \Sigma_{hkl}(||F_{o,\,hkl}| - |F_{c,\,hkl}||)/|F_{o,\,hkl}|$, where $F_{o,\,hkl}$ and $F_{c,\,hkl}$ are the observed and calculated structure factor amplitudes. $R_{free}$ is the same as $R_{cryst}$ but calculated over the 5% randomly selected fraction of the reflection data not included in the refinement.

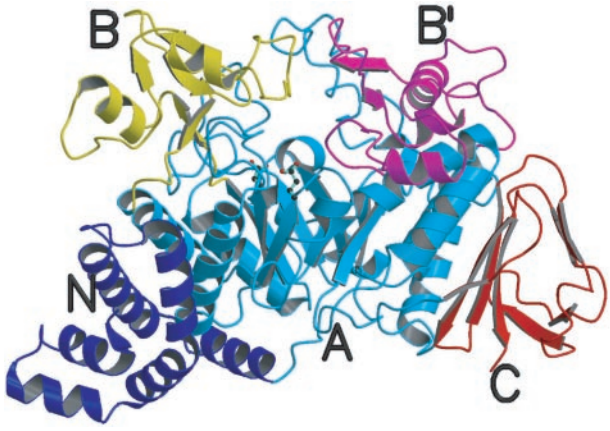


FIG. 1. **Schematic representation of the AS structure with labeling and color-coding of the five domains.** *N, dark blue*; *A*, *light blue; B, yellow; B′, magenta; and C, red*. The two catalytically active residues (Asp$^{286}$ and Glu$^{328}$) are also shown. They are located at the end of the barrel β-strand 4 and at the tip of β-strand 5, respectively. The figure was produced with MOLSCRIPT (36) and Raster3D (37).

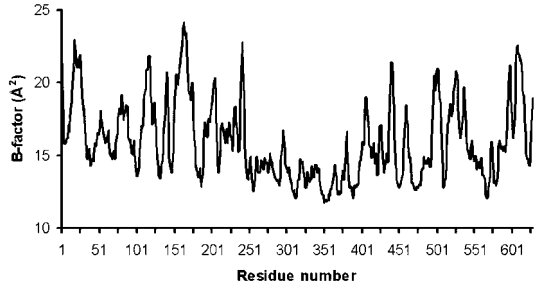


FIG. 2. **Plot of the AS Cα atom B-factors (Å$^2$).**

216–222) (Figs. 1 and 4). A B-domain is found in many α-amylases. In TAKA-amylase the main structural feature is a short three-stranded antiparallel β-sheet. There are also α-amylases that do not have a B domain. For example, barley α-amylase (30) has a short hairpin at this position.

Domain B′ (residues 395–460) starts with two α-helices (residues 400–407 and 410–422) (Figs. 1 and 4). They are followed by a short β-sheet (residues 433–436 and 446–449) where the strands are separated by a hairpin-like stretch of amino acid residues. A short α-helix (residues 451–456) terminates the domain. The domain starts immediately after two catalytically important residues (His$^{392}$ and Asp$^{393}$, see below) found in all related enzymes.

Domain C is an eight-stranded β-sandwich found C-terminal to the $(\beta/\alpha)_8$-barrel (residues 555–628). A C domain is found in other α-amylases, for example TAKA-amylase and barley α-amylase. Several of these domains are found in the CGTases, but so far the functional role of the C domain is unknown.

Although the complete AS sequence contains six cysteine residues no disulfide bridges are found in the structure. Some of the cysteines are exposed on the surface, but no tendency to multimerization has been reported.

The Cα displacement parameters (B-factors) are plotted in Fig. 2. The enzyme displays low overall thermal vibration with a mean B-factor for all atoms of 16.4 Å$^2$. The plot shows that especially the region 250–400 (from the start of h3 to the beginning of the B′ domain) has low displacement parameters and that the regions of the molecule with the highest displacement parameters are localized far from the substrate binding pocket.

*Relation to Family 13 Enzymes*—A comparison of the full-length enzyme with known protein structures using the DALI server (29) showed that the glycoside hydrolase Family 13 exo-acting enzyme oligo-1,6-glucosidase (31) had the highest similarity to AS. A total of 458 Cα atoms could be superimposed with an rms of 2.7 Å. The superimposable residues are almost all found in the A and C domains. The structural similarity to

Family 13 $\alpha$-amylases is also high. In particular, the TAKA-amylase-acarbose complex (32) had 368 superimposable C$\alpha$ atoms with a rms of 2.8 Å. A structural-based sequence alignment between TAKA-amylase, AS, and oligo-1,6-glucosidase starting after the unique N-domain is shown in Fig. 4. The boxed sequence patches represents regions of genuine structural similarity. Because of the high structural similarity the alignment can be used to propose AS-substrate interactions from enzyme-substrate investigations performed on related enzymes.

*Active Site Architecture*—The general acid residue Glu$^{328}$ and the nucleophile Asp$^{286}$ have been identified using conventional sequence alignment (9) and mutational studies (10). These results are supported by the structural alignment found in Fig. 4, which shows that the C$\alpha$ positions of the two residues coincides with catalytic residues from both TAKA-amylase and oligo-1,6-glucosidase. Asp$^{286}$ and Glu$^{328}$ are found at the tips of $\beta$-sheets 4 and 5 in the $(\beta/\alpha)_8$-barrel of AS (Fig. 1), as required for Family 13 members. The distance between Asp$^{286}$ C$\alpha$ and Glu$^{328}$ C$\alpha$ is 5.4 Å in accordance with AS being an $\alpha$-retaining enzyme (14). A Tris molecule is bound at the active site (Fig. 3) with a short hydrogen bond (2.6 Å) between O$\delta$2 of Asp$^{286}$ and one of the Tris oxygens and several hydrogen bonds to surrounding amino acid side chains (Asp$^{144}$, His$^{187}$, Glu$^{328}$, and Arg$^{509}$). Tris has previously been found to be a very good probe for the active site of $\alpha$-amylases (33).

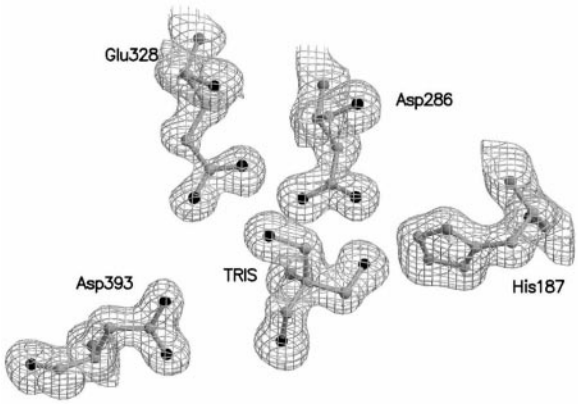


FIG. 3. **Drawing of the 1$\sigma$ 2Fo-Fc electron density around the active site of AS.**

The TAKA-amylase-acarbose complex (32) has identified a number of enzyme-substrate active site interactions. Around the −1 subsite the following interactions are reported (conserved residues at an equivalent position in AS given in parentheses): The nucleophile Asp$^{206}$ O$\delta$2 (Asp$^{286}$) is forming a hydrogen bond to the O6 of the I-ring of the modified acarbose (Fig. 5). His$^{122}$ (His$^{187}$) also forms a hydrogen bond to O6I. Arg$^{204}$ (Arg$^{284}$) forms a salt-bridge to the O$\delta$1 of the nucleophile and is very important for the correct positioning of the nucleophile. Arg$^{204}$ (Arg$^{284}$) has an additional weak hydrogen bond to O$^2$I. Glu$^{230}$ (Glu$^{328}$) is the general acid/base. It forms a hydrogen bond to the acarbose N. Asp$^{297}$ (Asp$^{393}$) O$\delta$1 and O$\delta$2 forms hydrogen bonds to O$^2$I and O3I respectively. Tyr$^{82}$ (Tyr$^{147}$) provides an important stacking platform for the substrate ring at the −1 position. Finally His$^{392}$ (His$^{296}$) forms a short hydrogen bond to the hydroxyl O of Tyr$^{82}$ (Tyr$^{147}$) an interaction suggested to be pivotal for the positioning of the stacking platform (32). All of these residues can be found at identical C$^{\alpha}$ positions in TAKA-amylase, AS, and oligo-1,6-glucosidase (Figs. 4 and 5). As seen in Fig. 5, the side chains of these residues are found in identical spatial positions as well. Thus $\alpha$-amylases and AS have very similar active site architecture with respect to the immediate surroundings of the scissile bond (subsite −1). This is in agreement with the general mechanism outlined in Scheme 1. The mechanism for the formation of the covalent intermediate is similar. But how does AS ensure specificity for sucrose as the first substrate, and how does AS

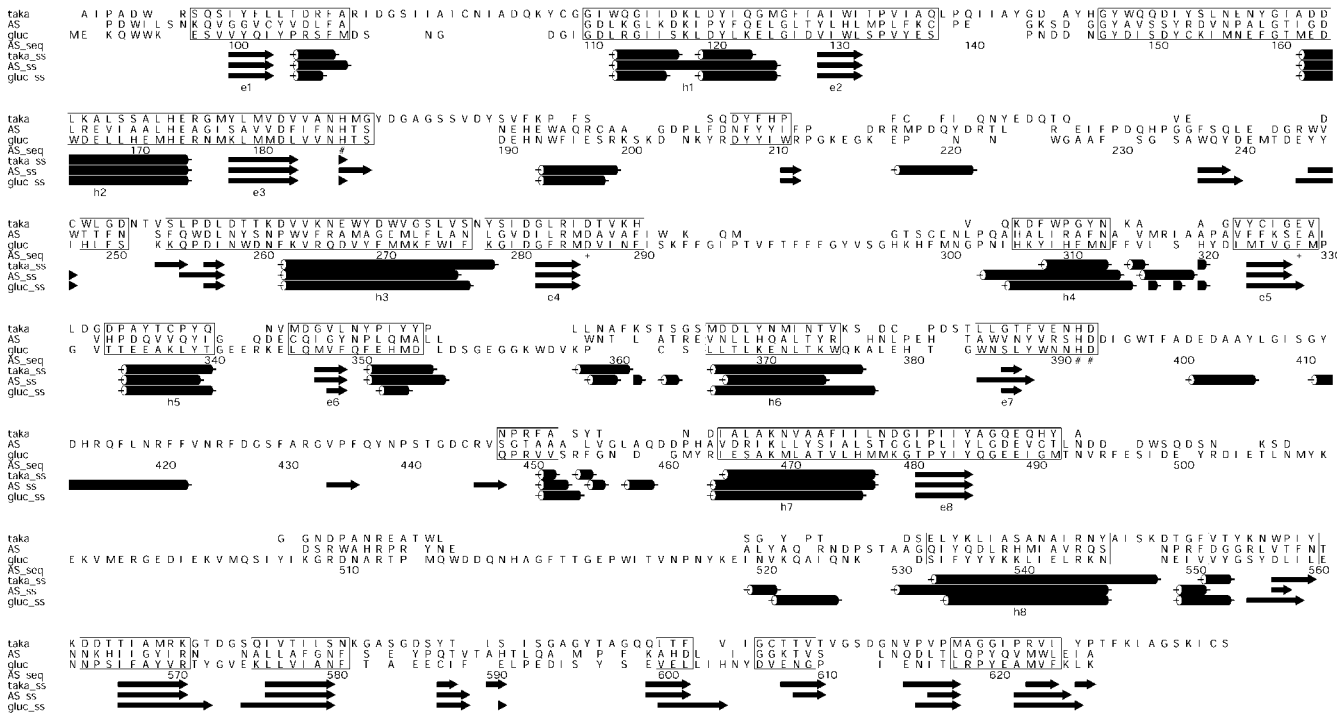

FIG. 4. **Structural alignment of members of Family 13 of the glucoside hydrolases.** *Taka,* $\alpha$-amylase from *A. oryzae*(18); *AS,* amylosucrase from *N. polysaccharea*; *gluc,* oligo-1,6-glucosidase from *B. cereus* (31). Stretches corresponding to genuine topological equivalence are *boxed* (38, 39). The AS sequence numbers (*AS_seq*) and the DSSP assignment of secondary structure elements are inserted (*taka_ss*, *AS_ss,* and *gluc_ss*)(28). The eight alternating $\beta$-sheets (e1–e8) and $\alpha$-helices (h1–h8) of the $(\beta/\alpha)_8$-barrel (domain A) are labeled. The two catalytically active residues Asp$^{286}$ and Glu$^{328}$ are indicated by a + whereas other important residues (His$^{187}$, His$^{392}$, and Asp$^{393}$) are marked by a #.

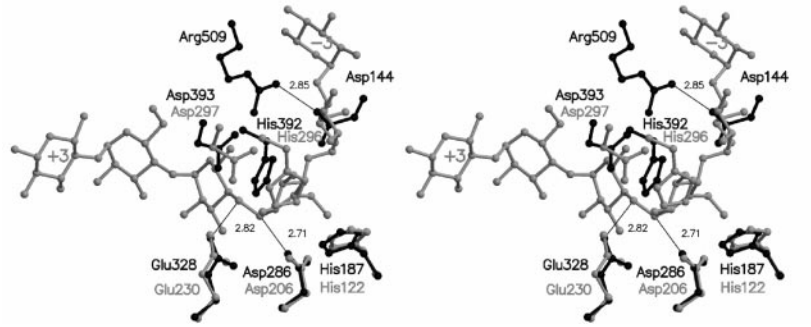


FIG. 5. **Stereo drawing of the superposition of the active sites of AS (*black*) and the TAKA-amylase-acarbose complex (*gray*).** Atoms in $Asp^{286}$ and $Glu^{328}$ were used to create the superimposition. The amino acid residue labels are *black* for AS and *gray* for TAKA-amylase. The elongated acarbose molecule is for clarity labeled at the +3 and −3 subsite. Distances (from the superimposition) between the nucleophile ($Asp^{286}$ Oδ1) and the anomeric carbon at subsite −1 in acarbose and between the general acid ($Glu^{328}$ Oϵ2) and acarbose N are shown (in Å). Furthermore, the distance (in Å) in the salt bridge found in AS between $Asp^{144}$ Oδ2 and $Arg^{509}$ Nη2 is shown.

prevent water from being the second substrate? These questions can be addressed by studying the superposition of AS and TAKA-amylase at the other subsites mapped out by the TAKA-amylase-acarbose complex.

*Specificity for Sucrose as the First Substrate*—TAKA-amylase is an endo-acting enzyme. It has a total of six specific binding sites for linked α-(1→4)-glucosyl moieties. The TAKA-amylase residues reported to be involved in enzyme-substrate contacts in subsites +1 and +2 are not structurally conserved in AS. TAKA-amylase $His^{210}$ in subsite +1 donating a hydrogen bond from Nϵ2 to O5J is a Phe in AS, whereas TAKA-amylase $Lys^{209}$ with hydrogen bonds to the modified acarbose hydroxyls OK2 and OK3 is an Ala in AS. This suggests that the +1 subsite in AS is modified to accommodate specificity for the furanosyl ring of sucrose.

The TAKA-amylase-2 subsite has been completely disrupted in AS. $Asp^{144}$ from loop2 forms a salt bridge with $Arg^{509}$ and thus occupies the subsite. An equivalent salt bridge is observed in the exo-acting oligo-1,6-glucosidase. An Ala and an Asp are found in these positions in TAKA-amylase. The salt bridges gives the active site a pocket topology in AS and oligo-1,6-glucosidase, in contrast to the cleft observed in TAKA-amylase. The result of the pocket topology is an exo-acting enzyme. The α-amylase cleft is closed by residues from domain B, domain B′, and loop2. The bottom of the pocket is quite thin-walled with a solvent accessible dent in the protein surface right behind the $Asp^{144}$–$Arg^{509}$ salt bridge. Without this blockage the active site topology would be a tunnel. In conclusion, the assumed furanosyl specificity at the +1 site and the salt bridge creates the sucrose specificity in AS.

*Oligosaccharides as Second Substrates*—The pocket topology in AS greatly reduces the solvent accessibility to the active site. When examining the AS structure superimposed with the TAKA-amylase-acarbose structure it can be seen that the pocket includes the −1 and +1 subsites. The superposition also suggests that $Phe^{250}$ is sandwiching the I-ring of the modified acarbose at the −1 subsite with $Tyr^{147}$ in AS. TAKA-amylase has a Gly at this position, oligo-1,6-glucosidase also have a Phe. This could implicate a more stable covalent intermediate in AS and oligo-1,6-glucosidase compared with α-amylases. This in turns could reflect the reduced accessibility of the active site. The intermediate simply has to exist long enough for the fructose to leave the active site and the second substrate (oligosaccharide or water) to enter.

The pyranosyl ring bound at the TAKA-amylase +2 subsite can just be seen in the surface plot (Fig. 6). Compared with the exo-acting hydrolase oligo-1,6-glucosidase the pocket of AS is very narrow leaving little room for water to enter when an oligosaccharide such as elongated acarbose is in the pocket. In

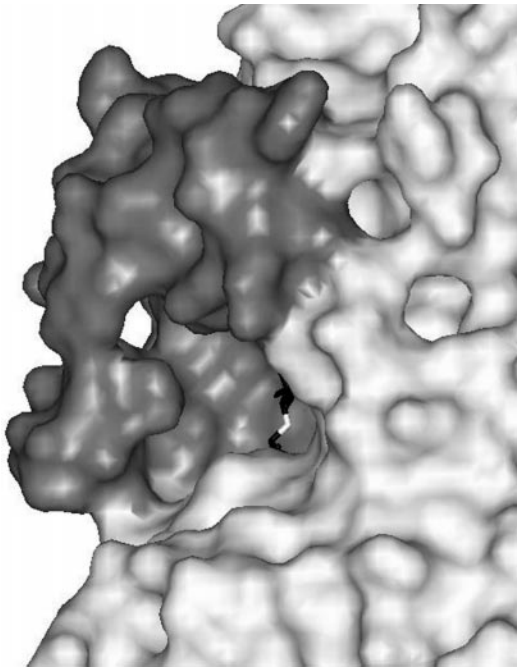

FIG. 6. **Drawing of the solvent accessible surface of AS near the pocket opening.** The B′-domain is colored *dark gray*. The O4L of the superimposed modified acarbose is colored *white* indicating the positions of the TAKA-amylase subsites.

the superimposition of acarbose into the AS structure the modified acarbose molecule fills the pocket almost completely. The surface area of the enzyme around the pocket-entrance is however quite open (Fig. 6). In fact several ravines in the surface leads to the pocket. Hence, it could be speculated that the growing glucan polymer is embedded in one ravine, whereas sucrose/fructose approaches/leaves the active site through another ravine. An architecture like this with a number of remote glucose binding subsites (securing a high "effective" concentration of the oligosaccharide chain) could be responsible for the transferase rather than hydrolase activity of AS. The unique AS domain-B′ is involved in the formation of these ravines (Fig. 6, *dark gray surface*). Because of the close proximity to the active site and the high content of aromatic residues (7 Phe, 3 Tyr, and 1 Trp out of 54 residues) it is tempting to propose that the B′-domain is essential for the binding of the growing glucan polymer. However, this hypothesis has to be tested by experiments involving complex formation with different oligosaccharides.

*Calcium Independence*—No calcium ions were found in the

structure. This also makes AS more similar to oligo-1,6-glucosidase than to TAKA-amylase. However, most of the $Ca^{2+}$ site arrangement found in many amylases is conserved. In TAKA-amylase a calcium ion is hepta-coordinated by oxygen atoms from $Asp^{175}$ (O$\delta$1 and O$\delta$2), $Asn^{121}$ (O$\delta$1), $Glu^{162}$ (backbone O), $His^{210}$ (backbone O), and three water molecules. For both AS and oligo-1,6-glucosidase the calcium ion found in $\alpha$-amylases is replaced with a presumable protonated lysine N$\zeta$ ($Lys^{293}$ in AS and $Lys^{206}$ in oligo-1,6-glucosidase). The two side chains involved in calcium binding ($Asn^{121}$ and $Asp^{175}$ in TAKA-amylase) are structurally conserved ($Asn^{186}$ and $Asp^{256}$) in AS. However, only $Asp^{256}$ O$\delta$2 is within hydrogen bonding distance of the TAKA-amylase $Ca^{2+}$ site. One of the backbone interactions (O from $His^{210}$ in TAKA-amylase) is also conserved in AS ($Phe^{290}$), but the change in side chain disables the interaction between the "calcium" site and the subsite +1 described for TAKA-amylase (32). The last of the three hydrogen bonds found for $Lys^{293}$ N$\zeta$ comes from a water molecule. The lack of calcium has also been observed in neopullulanase (34) and maltogenic $\alpha$-amylase (35).

*Acknowledgments*—We thank L. Jacobsen for help with the crystallization experiments and V. Stojanoff at BM 14 ESRF for help with the MAD data collection and processing.

REFERENCES

1. Hehre, E. J., and Hamilton, D. M. (1946) *J. Biol. Chem.* **166,** 777–778
2. MacKenzie, C. R., McDonald, I. J., and Johnson, K. G. (1978) *Can. J. Microbiol.* **24,** 357–362
3. Riou, J. Y., Guibourdenche, M., and Popoff, M. Y. (1983) *Ann. Microbiol.* **134B,** 257–267
4. White, O., Eisen, J. A., Heidelberg, J. F., Hickey, E. K., Peterson, J. D., Dodson, R. J., Haft, D. H., Gwinn, M. L., Nelson, W. C., Richardson, D. L., Moffat, K. S., Qin, H. Y., Jiang, L. X., Pamphile, W., Crosby, M., Shen, M., Vamathevan, J. J., Lam, P., McDonald, L., Utterback, T., Zalewski, C., Makarova, K. S., Aravind, L., Daly, M. J., Minton, K. W., Fleischmann, R. D., Ketchum, K. A., Nelson, K. E., Salzberg, S., Smith, H. O., Venter, J. C., and Fraser, C. M. (1999) *Science* **286,** 1571–1577
5. Nierman, W. C., Feldblyum, T. V., Laub, M. T., Paulsen, I. T., Nelson, K. E., Eisen, J., Heidelberg, J. F., Alley, M. R. K., Ohta, N., Maddock, J. R., Potocka, I., Nelson, W. C., Newton, A., Stephens, C., Phadke, N. D., Ely, B., DeBoy, R. T., Dodson, R. J., Durkin, A. S., Gwinn, M. L., Haft, D. H., Kolonay, J. F., Smit, J., Craven, M. B., Khouri, H., Shetty, J., Berry, K., Utterback, T., Tran, K., Wolf, A., Vamathevan, J., Ermolaeva, M., White, O., Salzberg, S. L., Venter, J. C., Shapiro, L., and Fraser, C. M. (2001) *Proc. Natl. Acad. Sci. U. S. A.* **98,** 4136–4141
6. Hehre, E. J. (1949) *J. Biol. Chem.* **177,** 267–279
7. Preiss, J., and Romeo, T. (1994) *Prog. Nucleic Acids Res. Mol. Biol.* **47,** 299–329
8. Buttcher, V., Welsh, T., Willmitzer, L., and Kossmann, J. (1997) *J. Bacteriol.* **179,** 3324–3330
9. Potocki De Montalk, G., Remaud-Simeon, M., Willemot, R. M., Planchot, V., and Monsan, P. (1999) *J. Bacteriol.* **181,** 375–381
10. Sarcabal, P., Remaud-Simeon, M., Willemot, R. M., Potocki De Montalk, G., Svensson, B., and Monsan, P. (2000) *FEBS Lett.* **474,** 33–37
11. Potocki De Montalk, G., Remaud-Simeon, M., Willemot, R., and Monsan, P. (2000) *FEMS Microbiol. Lett.* **186,** 103–108
12. Potocki De Montalk, G., Remaud-Simeon, M., Willemot, R. M., Sarcabal, P., Planchot, V., and Monsan, P. (2000) *FEBS Lett.* **471,** 219–223
13. Skov, L. K., Mirza, O., Henriksen, A., Potocki De Monatlk, G., Remaud-Simeon, M., Sarcabal, P., Willemot, R. M., Monsan, P., and Gajhede, M. (2000) *Acta Crystallogr. Sect. D.* **56,** 203–205
14. Davies, G., and Henrissat, B. (1995) *Structure* **3,** 853–859
15. Deleted in proof
16. Koshland, D. E. (1953) *Biol. Rev. Camb. Philos. Soc.* **28,** 416–436
17. Klein, C., and Schulz, G. E. (1991) *J. Mol. Biol.* **217,** 737–750
18. Matsuura, Y., Kusunoki, M., Harada, W., and Kakudo, M. (1984) *J. Biochem.* **95,** 697–702
19. Uitdehaag, J. C., Mosi, R., Kalk, K. H., van der Veen, B. A., Dijkhuizen, L., Withers, S. G., and Dijkstra, B. W. (1999) *Nat. Struct. Biol.* **6,** 432–436
20. Davies, G. J., Wilson, K. S., and Henrissat, B. (1997) *Biochem. J.* **321,** 557–559
21. Otwinowski, Z., and Minor, W. (1997) *Macromol. Cryst.* **276,** 307–326
22. Terwilliger, T. C., and Berendzen, J. (1999) *Acta Crystallogr. Sect. D.* **55,** 849–861
23. Cowtan, K., and Main, P. (1998) *Acta Crystallogr. Sect. D* **54,** 487–493
24. Perrakis, A., Morris, R., and Lamzin, V. S. (1999) *Nat. Struc. Biol.* **6,** 458–463
25. Jones, T. A., Zou, J. Y., Cowan, S. W., and Kjeldgaard, M. (1991) *Acta Crystallogr. Sect. A* **47,** 110–119
26. Brunger, A. T., Adams, P. D., Clore, G. M., DeLano, W. L., Gros, P., Grosse-Kunstleve, R. W., Jiang, J. S., Kuszewski, J., Nilges, M., Pannu, N. S., Read, R. J., Rice, L. M., Simonson, T., and Warren, G. L. (1998) *Acta Crystallogr. Sect. D* **54,** 905–921
27. Laskowski, R. A., MacArthur, M. W., Moss, D. S., and Thornton, J. M. (1993) *J. Appl. Cryst.* **26,** 283–291
28. Kabsch, W., and Sander, C. (1983) *Biopolymers* **22,** 2577–2637
29. Holm, L., and Sander, C. (1995) *Trends Biochem. Sci.* **20,** 478–480
30. Kadziola, A., Abe, J., Svensson, B., and Haser, R. (1994) *J. Mol. Biol.* **239,** 104–121
31. Watanabe, K., Hata, Y., Kizaki, H., Katsube, Y., and Suzuki, Y. (1997) *J. Mol. Biol.* **269,** 142–153
32. Brzozowski, A. M., and Davies, G. J. (1997) *Biochemistry* **36,** 10837–10845
33. Aghajari, N., Feller, G., Gerday, C., and Haser, R. (1998) *Structure* **6,** 1503–1516
34. Kamitori, S., Kondo, S., Okuyama, K., Yokota, T., Shimura, Y., Tonozuka, T., and Sakano, Y. (1999) *J. Mol. Biol.* **287,** 907–921
35. Kim, J. S., Cha, S. S., Kim, H. J., Kim, T. J., Ha, N. C., Oh, S. T., Cho, H. S., Cho, M. J., Kim, M. J., Lee, H. S., Kim, J. W., Choi, K. Y., Park, K. H., and Oh, B. H. (1999) *J. Biol. Chem.* **274,** 26279–26286
36. Kraulis, P. J. (1991) *J. Appl. Cryst.* **24,** 946–950
37. Merritt, E. A., and Bacon, D. J. (1997) *Macromol. Cryst.* **277,** 505–524
38. Russell, R. B., and Barton, G. J. (1992) *Proteins* **14,** 309–323
39. Barton, G. J. (1993) *Protein Eng.* **6,** 37–40